Yielding Behavior of Ceramic Matrix Composites

BHASKAR S. MAJUMDAR, GOLAM M. NEWAZ, and ALAN R. ROSENFIELD

Battelle Columbus Division, 505 King Avenue, Columbus, Ohio 43201, USA

ABSTRACT

The yielding of ceramic matrix composites is accompanied by the formation of many small matrix cracks. In this paper the growth of one such crack is analyzed, and the yield strength is defined as the stress level at which the stress needed for further propagation of the crack becomes constant. Under certain circumstances, particularly if the crack spacings are insufficient for ideal load transfer from matrix to fibers, the transition to a constant stress can occur discontinuously; and, this is associated with a flattened crack profile. The prediction of a discontinuity seems to be in agreement with the discontinuous nature of yielding that is observed experimentally. The paper also addresses some of the deficiencies in the mechanics and shear-lag analysis of earlier studies on ceramic composites.

KEYWORDS

Ceramic composites, cracks, displacements, fibers, matrix, mechanics, shear lag, stress intensity, yielding-type behavior

INTRODUCTION

The load-elongation curve for a fiber-reinforced ceramic matrix composite is similar to that for a steel. There is an initial linear elastic response, followed by an apparent yield point, where the load is nearly independent of displacement. Beyond this stage the deformation is non-linear and inelastic, until complete failure of the composite. This type of behavior contrasts with the deformation characteristic of a monolithic ceramic, for which there is a linear elastic response followed by catastrophic failure.

The yielding behavior that is observed on a macroscopic scale from the load-elongation curve, is microscopically associated with the material being traversed by a number of small cracks, similar to the twinning of metals. The cracks are restricted to the matrix material, and appear only at yielding. The fibers remain intact and bridge the crack surfaces. Unloading of the specimen beyond the yield point shows that the composite modulus has decreased, as further confirmation of cracking of the material at yielding. Consequently, from a micromechanical perspective the factors which control the formation of multiple matrix cracks are exactly those that control yielding.

The phenomenon of multiple matrix cracking has been addressed from a global energy viewpoint by Aveston, Kelly, and others [1,2]. The drawback of such an analyses is that the formulation depends on an inherent matrix strength (or strain), which is unclear for the composite. Marshall et al. [3,4] have modeled yielding of unidirectional ceramic-matrix composites by analyzing the growth of a single microcrack among the multitude of matrix cracks. It was hypothesized in the model that yielding occurred when the stress needed for further growth of the crack assymptotically approached a steady state value, independent of any further growth of the crack.

In this description [3,4], yielding is a rather continuous event, and should occur over a range of stress values. In contrast, most experiments on ceramic-matrix composites indicate that yielding is a discontinuous phenomenon, and occurs at a fixed level of stress for a particular system. Additionally, the model in [3,4] appears to have a number of other deficiencies, both in the mechanics of the individual crack, as well as in the shear lag analysis.

The model of yielding of an unidirectional ceramic-matrix composite, that is described in this paper, is similar to the approach of Marshall et al [3,4], in that it also focusses attention on the growth of an individual microcrack. The rationale is that what happens to a single crack is also what happens to any of the other matrix cracks, and consequently the growth behavior of the individual crack should be related to the macroscopically observed yielding phenomenon. The significant deviations from [3,4] are in the way the far-field applied stresses are related to the crack bridging stresses and displacements; also, the paper attempts to address some apparent discrepancies in the earlier shear lag analysis (see Appendix). It is shown that under particular circumstances yielding can occur discontinuously, when the crack shape changes from a parabolic type of profile to a flattened shape, as illustrated in Figure 1.

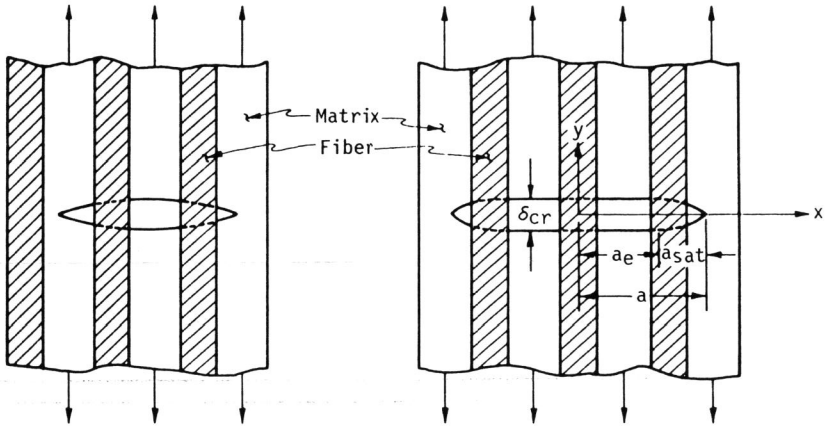

Fig. 1. Matrix cracking in ceramic composites. (a) Schematic of crack profile at low loads. (b) Flattened crack profile, when all the far field matrix stress, $\Delta\sigma^o_m$, is transferred to the fibers; the crack opening displacement displacement assumes a constant value, δ_{cr}.

Since the cracks are quite small, the analyses involves a blend of fracture mechanics and composite mechanics, similar to the blend [5,6] of fracture mechanics and dislocation theory in the case of plastically deformable solids. Far from the crack plane the fibers and matrix satisfy isostrain conditions, whereas near the crack surfaces the relative sliding of matrix and fibers occur at a constant value of friction stress. The assumption of constant friction stress is actually quite good, since recent electron microscopic

evidence [7] indicate that in a nicalon (SiC fiber)-glass ceramic composite, the fiber-matrix interface has a thin carbon layer, which allows easy relative movement between matrix and fibers.

ANALYSIS

Figure 2 shows a single matrix microcrack being loaded by the far-field applied stress (σapp). Let σ_f^o and σ_m^o correspond to the stress in the fibers and matrix respectively, far from the crack surfaces. Then, from the equilibrium of forces,

$$\sigma_{app} = \sigma_f^o V_f + \sigma_m^o V_m \quad (1)$$

where V_f and V_m are the volume fractions of fibers and matrix, respectively.

Because there is no relative sliding between fiber and matrix, σ_f^o and σ_m^o are related through the iso-strain relation

$$\sigma_f^o / E_f = \sigma_m^o / E_m = \sigma_{app} / E_c \quad (2)$$

where E_m, E_f, and E_c, are the elastic moduli of matrix, fiber, and composite, respectively. It is important to point out that equations 1 and 2 are only valid far from the crack surfaces.

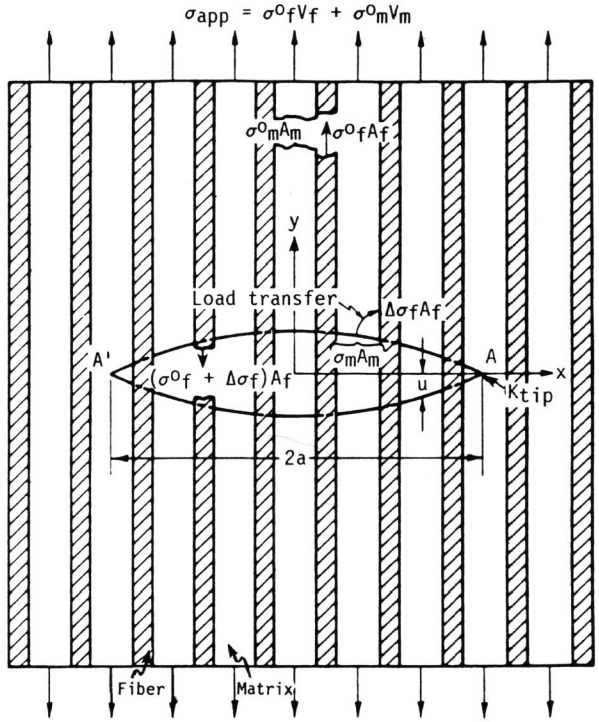

Fig. 2. Schematic, showing the details of matrix cracking and load transfer in ceramic matrix composites. For a specific value of opening, u, there is a corresponding increase, $\Delta\sigma_f$, in the fiber stress.

At the crack surface the matrix does not carry any load. Imagine that the crack is introduced in the following manner. Initially a cut is made in the matrix material (with the fibers remaining intact), but tractions are applied on the cut-surfaces to balance the applied load. As far as the deformation of the composite is concerned, nothing happens at this stage. Next, those tractions are gradually reduced to zero. During this process the matrix relaxes, and its elastic strains gradually reduce by amounts corresponding to the reduction in the tractions divided by E_m.

The reduction in strain in the matrix produces relative displacement of the adjacent cut surfaces. However, since the fibers remain intact, they cannot displace by the same extent. Consequently, there is relative sliding between fibers and matrix, with the matrix trying to pull away from the fibers. For an individual fiber the situation is as if the fiber was held in a grip, and the matrix was being stripped from the fiber, in a manner which is essentially the reverse of the familiar fiber pull-out experiment.

Because of the existence of a constant friction stress at the fiber-matrix interface, the relative sliding is limited; for a given amount of relative displacement, a part of the matrix stress, which originally existed near the cut surfaces, is transferred to the intact fibers. It is this load-transfer ability, through the friction stress, that makes the composites so forgiving. The shear lag analysis is described in Appendix A, and it provides a relation between the extent of relative sliding, u, and the corresponding amount of matrix load that is transferred to the fibers, or alternately, the additional stress in the fibers ($\Delta\sigma_f$) due to the load transfer. Because of symmetry at the crack surface, the displacement u is exactly half the crack opening displacement, δ.

It is assumed that the crack in the matrix propagates at a constant value of stress intensity factor, K_{tip}, which exists at the tips A or A' in Figure 2. The existence of a K_{tip} requires a parabolic type of elastic displacement (δ_{el}) profile for the crack surfaces. Additionally [8,9], there is a logarithmic type of inelastic displacement profile [10] which occurs due to the stretching of the individual ligaments (fibers), and these displacements exist even when K_{tip} is zero, as shown by Bilby, Cottrell, and Swinden [10]. However, since the entire matrix crack is bridged, these BCS type of displacements are small compared to the elastic displacements. Hence, the total crack opening displacement (COD), δ, is approximately equal to δ_{el}.

Displacements must be calculated because the stresses in the fibers, which bridge the crack surfaces, depend on the amount of transferred matrix loads; the latter, in turn, are controlled by the extent of relative sliding, u (= $\delta/2$). However, the matrix cannot transfer a stress greater than σ_m^o, which is the stress in the matrix far from the crack surfaces. Consequently, it follows from the shear lag analysis, that there must exist a maximum amount of relative displacement, u_{cr}, which depends critically on the value of σ_m^o. In other words, for a given applied stress, σ_{app}, the COD of the crack cannot increase without bound as the crack extends, but is cut-off at a maximum value, δ_{cr} (=$2u_{cr}$). It is this restriction that provides the flattened shape shown in Figure 1b.

The rest of the analyses is essentially a mathematical description of the above physical picture. The stress in the fibers at the crack surfaces is given by

$$\sigma_f = \sigma_f^o + \Delta\sigma_f \tag{3}$$

where, from the shear lag analysis of Appendix A, it follows that

$$\Delta\sigma_f = (2\Gamma/r)\ \{\ u/\pi r\Gamma\beta\ \}^{1/2} \tag{4}$$

Here, Γ is the friction stress between matrix and fibers, r is the radius of fibers, u is a function of x and is the relative total displacement (equal to half the crack opening displacement, δ) between the matrix and fibers , and

$$\beta = (1/E_mA_m) + (1/E_fA_f) \tag{5}$$

In the above equation, A_m and A_f (=πr^2) are the cross sectional areas of matrix and fibers, respectively, so that

$$V_f = A_f/(A_f + A_m) \tag{6}$$

The relative fiber-matrix displacement is half the COD for an elastic crack loaded to a stress intensity level K_{tip}, and, from reference [11] it follows that

$$u = 2\ K_{tip}\ \sqrt{a^2 - x^2}\ /\ E_c'\ \sqrt{\pi a} \tag{7}$$

where $E_c' = E_c/(1-\mu^2)$, and μ is the Poisson's ratio.

Figure 2 shows that the applied load (= $\sigma_m^o A_m + \sigma_f^o A_f$) is balanced by the load in the fibers (=$\sigma_f A_f$= [$\sigma_f^o + \Delta\sigma_f$] A_f), and the local K_{tip}, i.e.

$$K_{applied} = K_L + K_{tip} \tag{8}$$

where $K_{applied}$ is due to a constant far-field applied stress, σ_{app}, and K_L is the ligament contribution due to a stress, σ_{cs}, distributed on the crack surface. The stress, σ_{cs}, is related to the fiber stress ($\sigma_f^o + \Delta\sigma_f$) through the relation

$$\sigma_{cs} = (\sigma_f^o + h\Delta\sigma_f)\ V_f \tag{9}$$

since only an area-fraction V_f is occupied by the fibers. Implicitly it is assumed in equation 9 that the fiber stress is averaged out over the matrix-plus-fiber area on the crack surfaces. The constant h ($\leq$1) has been introduced into equation 9 to account for partial load transfer, which can occur if half the crack spacing (l_o) is less than the critial length (l_{cr}=$\{u/\pi r\Gamma\beta\}^{1/2}$) needed for ideal load transfer ($\Delta\sigma_f$), corresponding to relative displacement, u; thus, $h = l_o/l_{cr}$.

From fracture mechanics principles [11],

$$K_L = 2\sqrt{a/\pi} \int_0^a \sigma_{cs}\ dx\ /\ \sqrt{a^2-x^2} \tag{10}$$

or, using equations 4,7, and 9

$$K_L = 1.198\ \Omega\ a^{3/4} + \sigma_f^o V_f \sqrt{\pi a} \tag{11}$$

where Ω = 2.397 h $\{E_fK_{tip}\Gamma/(1+\Phi)rE_c'\}^{1/2}$ V_f , and $\Phi = E_fV_f/E_mV_m$

Now,

$$K_{applied} = \sigma_{app}\sqrt{\pi a} = \sigma_m^o V_m \sqrt{\pi a} + \sigma_f^o V_f \sqrt{\pi a} \tag{12}$$

Substituting equations 11 and 12 into equation 8, and substituting for σ_m^o from equation 2, we have

$$\sigma_{app} = c_1\ a^{1/4} + c_2/\sqrt{a} \tag{13}$$

where c_1 = 1.620 h $\{E_fK_{tip}\Gamma/(1+\Phi)rE_c'\}^{1/2}$ (E_c'/E_m) (V_f/V_m), and
$c_2 = K_{tip}\ (E_c'/E_m)/V_m\sqrt{\pi}$.

The behavior of equation 13 is shown by the upper curves in Figure 3, with the following set of material properties for a SiC reinforced glass-ceramic composite [3]: E_f=200 GPa, E_m=85 GPa, E_c=143 GPa, $V_f = V_m$=0.5, r = 8μm, Γ=2 MPa, and K_{tip}=2 MPa$\sqrt{m}$. Three values of h (namely, 1.0, 0.75, 0.5) have been used for the parametric curves. Here K_{tip} is taken to correspond to the fracture toughness, K_m (=2 MPa$\sqrt{m}$), of the unreinforced matrix. In view of the presence of other fibers and residual stresses, K_{tip} would probably be less than K_m.

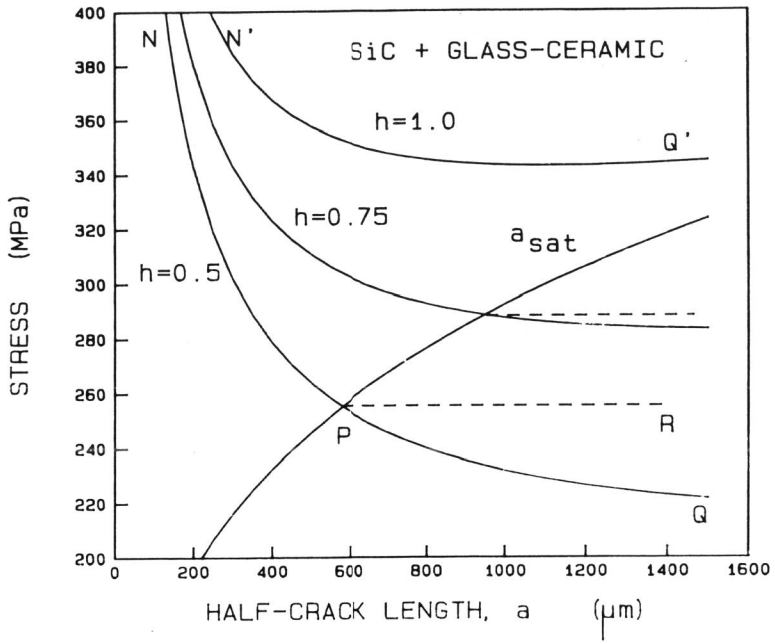

Fig. 3. Applied stress plotted versus half crack length, a. The equilibrium conditions for crack growth are represented either by the falling curves, or by the dashed lines, depending upon the value of a. The rising curve, a_{sat}, provides the critical crack lengths needed to obtain a flattened crack profile for particular values of applied stress. As an example, for h=0.5, the equilibrium condition is represented by the curve NP for $a < a_{sat}$ (i.e. to the left of P), and by the dashed line PR for $a > a_{sat}$.

Figure 3 shows that the stress needed to propagate the crack decreases rapidly at short crack lengths. If the load transfer is ideal (h=1), then the stress needed for crack growth assymptotically reaches a plateau level (actually a shallow minimum), and, similar to references [3,4], this would correspond to the yield stress.

For non-ideal load transfer, equation 13 can become invalid at long crack lengths, since, as already mentioned, the crack opening displacement cannot be larger than a value, δ_{cr}, which depends on the current value of σ_m^o, and hence on σ_{app} through equation 2. The maximum value of relative displacement between fibers and matrix (u_{cr}) is obtained by equating the matrix load far from the crack to the additional load in the fibers, since this corresponds to the maximum load that can be transferred. Thus,

$$\sigma_m^o \, A_m = \Delta\sigma_f \, A_f \qquad (14)$$

For crack spacings less than $2l_{cr}$, the constant h would be multiplied on both sides of equation 14, and would cancel out. Using the shear lag analysis, equation 4, and substituting $\sigma_m^o = (E_m/E_c')\sigma_{app}$ from equation 2, we have

$$u_{cr} = \{(1+\Phi)/\Phi^2\} \{\sigma^2_{app}/4\Gamma E_f\} \{E_f/E_c'\}^2 \, r \qquad (15)$$

For a given applied load, the crack length (a_{sat}) at which u_{cr} is just reached is obtained by equating equations 7 and 15, with x=0. Hence,

$$a_{sat} = (\pi/64) \, [\{(1+\Phi)/\Phi^2\} \{E_f/E_c'\} \{\sigma^2_{app} \, r / K^2_{tip}\} \{K_{tip}/\Gamma\}]^2 \qquad (16)$$

The lower solid curve in Figure 3 corresponds to equation 16, and provides critical values of crack lengths (a_{sat}) for various applied stresses. At a given applied stress, if the crack length is greater than the that specified by the curve, the crack will have a profile as shown in Figure 1b.

Figure 3 shows that the force-equilibrium curve can intersect the a_{sat} curve at a point such as P, and beyond this crack length equation 14 is no longer valid. After the intersection point, the appropriate crack surface stresses, using the notation of Figure 1b, are

$$\sigma_{cs} = (\sigma_f^o + h\Delta\sigma_f) V_f = \sigma_f^o V_f + h\sigma_m^o V_m \quad \text{for} \quad x \leq a_e \qquad (17a)$$
$$= (\sigma_f^o + h\Delta\sigma_f) V_f \quad \text{for} \quad a_e \leq x \leq a \qquad (17b)$$

In deriving equation 17a we have used equation 14, since over this range of x values, all the load is transferred from the matrix to the fibers. On the other hand equation 17b is identical to that used for deriving equation 11. Substituting equations 17a and 17b into equation 10, we have

$$K_L = 2\sqrt{a/\pi} \left\{ \int_0^{a_e} (\sigma_f^o V_f + h\sigma_m^o V_m) dx/\sqrt{a^2-x^2} + \int_{a_e}^{a} \sigma_{cs} \, dx \, /\sqrt{a^2-x^2} \right\} \qquad (18)$$

Here, $a_e = a - a_{sat}$, where a_{sat} is obtained from equation 16.
Substituting into the main equilibrium equation 8, it can be shown that

$$\sigma_{app} = 1.311 h c_1 a^{1/4} f_1 / \cos^{-1}(a_e/a) + 1.57 c_2 \, /(\sqrt{a} \cos^{-1}(a_e/a) \qquad (19a)$$

where,

$$f_1 = \sqrt{2} \, F(\theta, 1/\sqrt{2}) - 2\sqrt{2} \, E(\theta, 1/\sqrt{2}) + 1.198 \qquad (19b)$$

F and E are incomplete elliptic integrals of the first and second kind respectively with modulus $1/\sqrt{2}$,

$$\sin\theta = \sqrt{2} \sin(\pi/4 - \alpha/2) \qquad (19c)$$
$$\alpha = \cos^{-1}(a_e/a) \qquad (19d)$$

It can then be shown that 'a' satisfies the following equation

$$a = (g_1/g_2)^{4/3} \qquad (20)$$

where
$g_1 = 1.198 \, c_2/c_1$, and, $g_2 = (a_{sat}/a)^{1/4} \cos^{-1}(1 - a_{sat}/a) - h f_1$

From equation 20 the values of a can be obtained for various values of a_{sat}/a. The value of a at $a_{sat}/a = 1$ determines the intersection of the two curves shown in Figure 3. Substituting into equation 19a, the corresponding values of applied stresses can be obtained.

The dashed curves in Figure 3 show the variation of the applied stresses with crack length, beyond the point of intersection. The stress stabilizes to a constant value, and all that occurs during this period is a stretching of the zone of constant displacement. Most importantly, the transition to a constant stress occurs discontinuously, which agrees with the discontinuous nature of yielding.

The yield point of the material has been measured, and it is approximately 290 MPa, whereas the present calculations (Figure 3) indicate that it can vary between 250 MPa and 340 MPa, depending on the value of h. Observed [4] crack spacings ($2l_c$) for this material is approximately 400 μm. On the other hand, using equations 14, 4, and the second half of

equation 2, and replacing the bracketed term in equation 4 by l_{cr}, and assuming the applied stress is 300 MPa, the value of l_{cr} is approximately 360 μm. Thus, $h = l_o/l_{cr} \approx 0.56$, Hence, the lowest equilibrium curve in Figure 3 is most appropriate for the material. The figure shows that the transition to a flattened crack profile should occur at a≈580 μm, and the corresponding yield stress should be approximately 250 MPa. In the case of a carbon-fiber reinforced glass composite [4], the trasnsition is found to occur at a≈ 80μm.

DISCUSSION AND CONCLUSIONS

A fracture mechanics based approach was used to analyze the yielding behavior of ceramic matrix composites. It was shown that the matrix cracking behavior could be conveniently conceptualized as the process of stripping of the matrix from the intact fibers. In this way the stresses in the fibers at the crack surfaces could be estimated in a consistent fashion.

It was shown that the maximum load transfer from the matrix to the fiber was equal to $\sigma_m{}^o A_m$, and this necessitated the attainment of a maximum crack opening displacement (δ_{cr}). For a given applied stress, there was a specific crack length ($2a_{sat}$), beyond which the crack attained a flattened proifile. This is consistent with micrographs [3], which show matrix cracks with constant crack opening displacements, rather than cracks with varying crack opening displacements, which are characteristic of unligamented cracks.

Similar to previous analyses, yielding was assumed to occur when the stress needed for further propagation of the crack became independent of crack length. The effect of neighboring cracks was introduced through the factor h, which depended on the available crack spacings. This approach may be over-simplistic, but it nevertheless provided significant insights. Thus, it was found that if crack spacings were too small, then the stress needed for further propagation of the crack became suddenly constant, rather than reaching a constant value assymptotically. This may explain why yielding is generally discontinuous, occuring at one specific value of applied stress, rather than being continuous, and occuring over a range of stress values.

The value of crack length (a≈580 μm) at which the transition occurred for the SiC reinforced glass ceramic, does appear too high, in comparison to the size of as-processed flaws. Part of the reason may be that residual stresses were not taken into account, and also some debonding could have occurred. Detailed calculations are now in progress. However, the value of a_{sat}=80 μm that was obtained for a carbon fiber reinforced composite appears realistic of as-processed flaw size, and provides confidence to the analysis.

ACKNOWLEDGMENTS

This work was partially supported by Battelle's internal funds. We thank Dr. John Holbrook for his encouragement in conducting these basic research activities.

REFERENCES

1. Aveston, J. and A. Kelly (1973). Theory of Multiple Fracture of Fibrous Composites. J. Mat. Sc., 8, p.352-362.
2. Aveston, J., G.A. Cooper and A. Kelly (1971). Single and Multiple Fractures. Properties of Fiber Composites. IPC Science and Technology Press Limited, England, pp.15-26.
3. Marshall, D.B. and A.G. Evans (1986). The Tensile Strength of Uniaxially Reinforced Ceramic Fiber Composites. In: Fracture Mechanics of Ceramics (R.C. Bradt, A.G. Evans, D.P.H. Hasselman and F.F. Lange,ed.), Vol.7, pp.1-15. Plenum Press, New York
4. Marshall, D.B., B.N. Cox, and A.G. Evans (1985). The Mechanics of Matrix Cracking in Brittle-Matrix Fiber Composites. Acta Metall., 11, pp.2013-2021.

5. Majumdar, B.S. and S.J. Burns (1981). Crack Tip Shielding - An Elastic Theory of Dislocations and Dislocation Arrays Near a Sharp Crack. Acta Metall., 29, pp.579-588.
6. Majumdar, B.S. and S.J. Burns (1983). A Griffith Crack Shielded by a Dislocation Pileup. Int. J. of Fracture, 21, pp.229-240.
7. Katz, A. (1988). Ceramic Matrix Composites. Presentation at the Ohio State University
8. Majumdar, B.S., A.R. Rosenfield and W.H. Duckworth (1988, in press). Analysis of R-Curve Behavior of Non-Phase-Transforming Ceramics. Engg.Fract. Mech., in press.
9. Majumdar, B.S., G.M. Newaz and A.R. Rosenfield (1988). Crack Bridging Behavior in Widely Different Materials, and a Generalized Approach to Their Analysis. Manuscript to be submitted for publication shortly.
10. Bilby, B.A., A.H. Cottrell, and K.H. Swinden (1963). The Spread of Plastic Yield from a Notch. Proc. Roy. Soc. A272, pp.304-314.
11. Broek, D. (1978). Elementary Engineering Fracture Mechanics, Sijthoff and Noordhoff International Publishers, Holland.

APPENDIX - A : SHEAR LAG ANALYSIS

Consider Figure A-1 (a), which shows a single fiber and its associated matrix. The area enclosed by AABB is within a short distance from the crack plane (assumed to be on the right hand side of BB), and shear lag is assumed to occur here by the relative sliding of fiber and matrix. On the left of AA there is no shear lag, and the stresses in the fibers and matrix are $\sigma_f{}^o$ and $\sigma_m{}^o$ respectively, and satisfy iso-strain conditions given by equation 2 of this paper. In region AABB iso-strain conditions are not valid. Let the stresses at the plane BB, in the fiber and matrix, be σ_f and σ_m, respectively. Because of unequal loads in fiber and matrix, there is different stretching, v_f and v_m, of fiber and matrix, respectively. The difference, (v_f-v_m), is equated to the relative displacement, u.

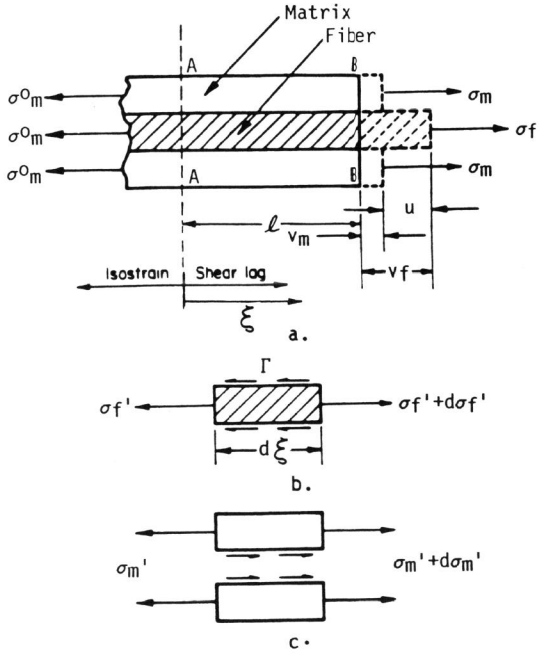

Fig. A-1. Shear lag analysis. (a) Deformed and undeformed unit fiber/matrix cell. (b) Fiber stresses. (c) Matrix stresses.

A segment of length $d\xi$ is removed from within the region AABB. The free bodies for the fiber and matrix are shown separately by Figures A-1(b) and A-1(c) respectively. The magnitudes $d\sigma$ represent incremental differences in stresses between the two faces. The shear stress Γ is constant at the interface, and it opposes sliding of the fiber from the matrix. The radius of the fiber is r, and its area is $A_f=\pi r^2$. Let the difference in displacements between the two faces of the length $d\xi$ be represented by v. Then, noting that $\sigma_f=\sigma_f^o$ and $\sigma_m=\sigma_m^o$ at $\xi=0$, it is easy to show that

$$dv_f/d\xi = \sigma_f'/E_f = 2\pi r\Gamma\xi/A_fE_f + \sigma_f^o/E_f \qquad (A\text{-}1)$$

$$dv_m/d\xi = \sigma_m'/E_m = -2\pi r\Gamma\xi/A_mE_m + \sigma_m^o/E_m \qquad (A\text{-}2)$$

where σ_f' and σ_m' are the stresses at any position, ξ. Integrating, with the boundary conditions that $v_f=v_m=0$ at $\xi=0$, we have at $\xi=\ell$ the following result,

$$u = \pi r\Gamma\{(1/E_fA_f)+(1/E_mA_m)\}\ell^2 + \{(\sigma_f^o/E_f) - (\sigma_m^o/E_m)\}\ell \qquad (A\text{-}3)$$

The terms in the second curly brackets equate to zero (equation 2 of this paper). Substituting $\xi=\ell$ in equation A-1, and substituting for ℓ from equation A-3, we obtain

$$\Delta\sigma_f = \sigma_f - \sigma_f^o = (2\Gamma/r)\ \{\ u/\pi r\Gamma\beta\ \}^{1/2} \qquad (A\text{-}4)$$

Equation A-4 provides the relation between the extra stress in the fiber, and the relative sliding u (between fiber and matrix) in the shear lag zone; it is equation 4 of the main text. Equation A-4 is valid only up to a critical displacement, such that $\Delta\sigma_fA_f$ is less than or equal to $\sigma_m^oA_m$. Beyond that point the displacement and load transferred are constant and independent of the position, x, of Figure 2; and $\Delta\sigma_f$ is obtained through Equation 14 of the main body of the text.

The relation between the load transferred and the displacement, u, that is derived in equation A-4, is significantly different from that in the literature [3,4]. In equation (A2) of reference [4] it was assumed that all the stress in the matrix, namely σ_m^o, was always transferred to the fibers, so that it follows from their equations (A2) and (A3) that the fiber stress at the crack plane also should be a constant, independent of the displacement, u. Although the final equation that is derived in the appendix of reference [4] shows a relation between the stress in the fibers and u, the displacement is actually determined as a constant, dependent only on the far field stresses, and cannot be allowed to vary with the value of K_{tip}, or the distance behind the crack tip.

The current shear lag analysis differs from the one in [4] primarily in that it is assumed that the load transferred is only a function of the relative displacement, u, independent of whether all the load in the matrix ($\sigma_m^oA_m$) can be transmitted to the fibers. At positions behind the crack tip where critical displacements have not been reached, only partial matrix load is transferred to the fibers. The remaining matrix load, because of the traction-free crack surface, is transferred to the matrix ahead of the crack tip. This is similar to what occurs for a monolithic material containing a crack, and it is the load transmission that produces the stress intensity factor. The current shear lag analysis also is consistent with the main body of the text, in that the displacements, u, are associated with the critical stress intensity, K_{tip}, for the matrix crack. In case all the load in the matrix were always transmitted to the fibers, independent of u, then K_{tip} would be zero, and ever increasing loads would be necessary to cause further matrix cracking. Such is contrary to experimental evidence.

It is important to recognize that the shear lag analysis is a simplified analysis of the complex processes that take place at the crack tip, and a more accurate finite element analysis is probably needed to determine the load distribution among the bridged fibers.